AD-A237 085

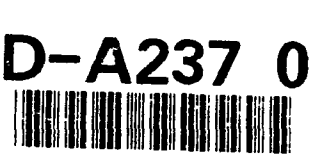

(2)

OFFICE OF NAVAL RESEARCH

Contract N00014-88-k-0482, Mod/Amend P00001

Technical Report No. 11

Mechanistic Investigations of Nanometer-Scale Lithography at Liquid-Covered Graphite Surfaces

by

Reginald M. Penner, Michael J. Heben and Nathan S. Lewis

DTIC COPY INSPECTED 5

Published in

Applied Phys. Lett. (1991) **58**, 1389

California Institute of Technology
Department of Chemistry
Pasadena, California 91125

May 31, 1991

A-1

Reproduction in whole or in part is permitted for any purpose of the United States Government.

This document has been approved for public release and sale; its distribution is unlimited.

91-02563

91 18 141

REPRODUCED AT GOVERNMENT EXPENSE

SECURITY CLASSIFICATION OF THIS PAGE

REPORT DOCUMENTATION PAGE

1a. REPORT SECURITY CLASSIFICATION Unclassified	1b. RESTRICTIVE MARKINGS
2a. SECURITY CLASSIFICATION AUTHORITY	3. DISTRIBUTION/AVAILABILITY OF REPORT Approved for Public Release and Sale. Distribution Unlimited
2b. DECLASSIFICATION/DOWNGRADING SCHEDULE	
4. PERFORMING ORGANIZATION REPORT NUMBER(S) ONR Technical Report #11	5. MONITORING ORGANIZATION REPORT NUMBER(S)
6a. NAME OF PERFORMING ORGANIZATION Nathan S. Lewis Caltech 6b. OFFICE SYMBOL (*If applicable*)	7a. NAME OF MONITORING ORGANIZATION
6c. ADDRESS (*City, State, and ZIP Code*) M.S. 127-72, Dept. of Chem. California Institute of Technology Pasadena, California 91125	7b. ADDRESS (*City, State, and ZIP Code*)
8a. NAME OF FUNDING/SPONSORING ORGANIZATION Office of Naval Research 8b. OFFICE SYMBOL (*If applicable*)	9. PROCUREMENT INSTRUMENT IDENTIFICATION NUMBER N00014-88-k-0482, Mod/Amend P00001
8c. ADDRESS (*City, State, and ZIP Code*) Attn. Code 413 800 N. Quincy St. Arlington, VA 22217	10. SOURCE OF FUNDING NUMBERS PROGRAM ELEMENT NO. / PROJECT NO. / TASK NO. / WORK UNIT ACCESSION NO
11. TITLE (*Include Security Classification*) Mechanistic Investigations of Nanometer-Scale Lithography at Liquid-Covered Graphite Surfaces	
12. PERSONAL AUTHOR(S) Reginald M. Penner, Michael J. Heben and Nathan S. Lewis	
13a. TYPE OF REPORT Technical 13b. TIME COVERED FROM June 90 TO June 91	14. DATE OF REPORT (*Year, Month, Day*) 1991, May 31 15. PAGE COUNT 18
16. SUPPLEMENTARY NOTATION	
17. COSATI CODES FIELD / GROUP / SUB-GROUP	18. SUBJECT TERMS (*Continue on reverse if necessary and identify by block number*) STM, Electrochemistry

19. ABSTRACT (*Continue on reverse if necessary and identify by block number*)

ABSTRACT: Pulse-induced nanometer-scale lithography has been performed on graphite surfaces that are in contact with pure water or other organic liquids. Very reproducible control over the pit diameter was observed in aqueous solutions, and a well-defined voltage threshold (4.0±0.2V) was also apparent. Near the threshold voltage, 7 Å dia. x 2 Å high protrusions were formed, while larger initial pulse voltages resulted in pits of diameter >20 Å. The protrusions were stable to imaging, but could be transformed into pits with the application of a subsequent voltage pulse. These protrusions are probable metastable intermediates in the pit formation process that operates both in liquid and gaseous ambients.

20. DISTRIBUTION/AVAILABILITY OF ABSTRACT ☒ UNCLASSIFIED/UNLIMITED ☐ SAME AS RPT ☐ DTIC USERS	21. ABSTRACT SECURITY CLASSIFICATION Unclassified
22a. NAME OF RESPONSIBLE INDIVIDUAL	22b. TELEPHONE (*Include Area Code*) / 22c. OFFICE SYMBOL

Mechanistic Investigations of STM Lithography at Liquid-Covered Graphite Surfaces

Reginald M. Penner, Michael J. Heben, and Nathan S. Lewis[a)]

Division of Chemistry and Chemical Engineering

California Institute of Technology

Pasadena, CA 91125

Calvin F. Quate

Edward Ginzton Laboratory

Department of Applied Physics

Stanford University

Stanford, CA 94305

ABSTRACT: Pulse-induced nanometer-scale lithography has been performed on graphite surfaces that are in contact with pure water or other organic liquids. Very reproducible control over the pit diameter was observed in aqueous solutions, and a well-defined voltage threshold (4.0±0.2V) was also apparent. Near the threshold voltage, 7 Å dia. x 2 Å high protrusions were formed, while larger initial pulse voltages resulted in pits of diameter >20 Å. The protrusions were stable to imaging, but could be transformed into pits with the application of a subsequent voltage pulse. These protrusions are probable metastable intermediates in the pit formation process that operates both in liquid and gaseous ambients.

Recently, atomic and molecular scale features have been produced on surfaces using scanning tunneling microscopy (STM) methods (1-6). At room temperature, the smallest permanent lithographic process reported to date involves the formation of ≈ 40 Å diameter, ≈ 3 Å deep pits on a highly ordered pyrolytic graphite (HOPG) surface (1). These pits were formed by the application of 3-8 V pulses of 10-100 μs duration, while maintaining a tunneling current. Although a substantial fraction of the STM tips successfully generated hundreds of uniform, 20-40 Å diameter pits when subjected to a train of constant amplitude and constant duration bias pulses(1), the pulse threshold at which the smallest features were observed varied substantially from tip to tip. Additionally, the lithography process was observed to require a humid atmosphere and to exhibit daily fluctuations in pulse bias vs. pit size. In order to elucidate the chemistry of this process, we have performed STM-lithography studies of HOPG surfaces in contact with water and other organic liquids. For HOPG in $H_2O(l)$, we have observed a well-defined pulse threshold of (4.0±0.2)V, which reproducibly yielded 7 Å diameter, 2 Å high protrusions. Larger voltage pulses yielded pits (with slightly larger dimensions) that were similar to those produced in air or in humid $N_2(g)$ atmospheres. This work demonstrates that sub-nanometer scale lithography can be accomplished on graphite at room temperature, and that STM studies can provide mechanistic information into the chemistry of the liquid-coated and gas-phase lithographic processes.

A STM specifically designed for imaging surfaces immersed in liquids was employed for this work (7). When imaging under solution, the quartz base of the microscope was filled with 2 mL of the desired liquid. Other procedures were standard for STM experiments. Bias pulses with a duration of 20 μs and an amplitude, E_p, of between 1 and 20 V (of the tip relative to the sample) were generated using a Wavetek model 802 pulse generator; most studies were performed with the tip negative relative to the sample, although qualititatively similar behavior was observed with the opposite polarity. STM data was acquired in the constant current mode at an X scan frequency (fast scan direction) of 10-20 Hz. The resulting tip height vs. position data were displayed as images either in conventional constant current fashion, or in

a derivative mode where changes in the height of the tip with respect to the sample were plotted versus position. The derivative mode facilitated analog electronic imaging of the rough surfaces produced by the lithography experiments. No additional filtering, smoothing or temporal averaging of the data was performed. The position dependent STM data was mapped into a 256 x 256 x 8-bit grey scale using an Arlunya TF5000 Video Image Processor, and was stored on a super-VHS video tape. The figures in this work were displayed as isolated frames on a 700 line video monitor and then were photographed for reproduction. Piezo calibration in the X and Y directions was accomplished using atomic resolution images of the HOPG surface as a distance scale. Calibration of the Z direction (normal to the surface) was derived from the piezo manufacturer's specifications for the tubular piezo crystal and was corroborated using laser interferometry measurements.

Tungsten wires that had been electrochemically etched were used as the STM tips. After etching, tips employed for imaging experiments in liquids were insulated with poly(α-methyl styrene) (30,000 g/eq. MW, Aldrich) from a 30 w/v% solution of the polymer in CH_2Cl_2 (8). Before STM imaging under liquids, the polymer-coated tungsten tips were then loaded into the STM and subjected to a "field emission" process at a bias of +15 V in air, in order to expose a small portion of metal tip for use in STM experiments(8). Experiments in pure $N_2(g)$ ambients were performed in a plexiglas glove box that was purged for 1 hr with dry $N_2(g)$ before imaging was initiated. Water (18 MΩ-cm resistivity) was obtained from a Nanopure water purification system. Rigorously dry toluene was obtained by distillation from CaH_2 in $N_2(g)$ followed by a second distillation, immediately prior to imaging, from $(\eta\text{-}C_5H_5)_2Ti$. Other organic solvents were of reagent grade and were used as received.

Figure 1 shows a series of constant height, derivative mode STM images of HOPG in contact with $H_2O(l)$. The tip scan direction during data acquisition was from right-to-left. Bright regions corresponded to movement of the tip away from the surface, while dark regions indicated tip movement toward the surface. Figure 1a shows a defect-free region of the graphite surface prior to the application of a bias pulse, and Figure 1b shows an image of the identical

region at reduced sensitivity. Images similar to Figure 1a and 1b served as a baseline for the area in which the desired lithographic feature was to be formed.

Application of a 20 μs duration -4.0 V amplitude bias pulse while tunneling to the H_2O(l)-covered graphite surface of Figure 1a,b resulted in the derivative mode image of Figure 1c. As the tip traversed the feature in Figure 1c from right-to-left, the signal generated was bright then dark, which indicated a protrusion in the surface topography. The absence of apparent atomic resolution in this (and subsequent) images derives from the fact that the reduced sensitivity of Figure 1b was required to image regions of the graphite surface that exhibited a height range (i.e. a dynamic range) greater than the 2 Å corrugation characteristic of clean graphite. Cross sections of the feature in Figure 1c revealed that it was 7 Å in diameter and approximately 1 Å in height (Figure 1d). Domed features like that shown in Figure 1c,d could be generated using >90% of the tips employed for lithography in H_2O(l) with $E_p = \pm(3.8\text{-}4.2$ V). These domes were stable to imaging at biases as high as ±500 mV for periods of >1 hr under the H_2O(l) ambient.

The protrusions in Figure 1c,d were only formed on graphite surfaces that were in contact with liquid H_2O, and only with pulses near the observed threshold voltage. Incrementally larger bias pulse amplitudes of $E_p = \pm(4.3\text{-}4.4)$V produced pits that were qualitatively identical to those observed for lithography on HOPG in air (1,2). As shown in Figures 1e and 1f, the diameter of a typical pit formed with a -4.2 V pulse under H_2O(l) was 40 Å, and its depth was 3 Å. Note that the darker region now appears first in the right-to-left scan direction of Figure 1e, which is the expected signal for a depression in the surface. The depth of the pit is consistent with the removal of a single graphite layer, as proposed earlier for bias-pulse lithography on HOPG in gaseous ambients (1,2). Further increases in the bias pulse amplitude resulted in monotonic increases in the dimensions of the resulting pit. As a representative example, Figures 1g and 1h show a derivative mode STM image and cross sections of an 80 Å diameter pit that was generated with a tip bias pulse amplitude of -4.5 V for HOPG in contact with H_20(l).

The reproducibility of bias-pulse lithography in $H_2O(l)$ improved in two distinct ways relative to the process in an air ambinet. The reproducibility of the threshold voltage (i.e, the voltage required to produce the smallest observed features) was observed to be (4.0 ± 0.2) V in $H_20(l)$ for a large number of independent experiments with a variety of STM tips. In contrast, experiments in laboratory air exhibited substantial daily variations of as much as 5 V in the pulse threshold, presumably due to variations in the relative humidity (9). Secondly, in $H_2O(l)$ the relationship between E_p and the pit (or dome) diameter was very well defined for pulse amplitudes above E_p. Figure 2 shows statistics relating E_p to the feature diameter; these statistics were obtained using 10 polymer-coated tungsten tips that were fabricated and used in STM-lithography experiments over the period of a week. The increased reproducibility obtained in $H_2O(l)$ underscores the link between the chemistry of the lithography process and the presence of water during the pulse period.

Several different ambients were investigated in order to confirm the suggestion that H_2O is required to form etch pits. At graphite surfaces in contact with either dry toluene(l) or dry $N_2(g)$, features could not be generated even with pulse amplitudes as large as ±10 V. However, introduction of H_2O into either of these ambients restored the ability to produce the features represented in Figure 1c,d. These observations are consistent with those of Terashima *et al.* (2) who observed a suppression of pit formation on graphite in 10 mtorr toluene vapor and in dry $N_2(g)$ ambients. Reagent grade organic solvents which were not rigorously dried, such as n-octane and mineral oil, behaved qualitatively like an air ambient. In these impure liquids, variations of the threshold voltage of up to several volts were observed, but in all cases lithography was facilitated at $|E_p| < 10$ V . In these ambients, the lithography operation yielded only pits, as was observed for experiments in an air ambient.

For graphite surfaces in contact with $H_2O(l)$, the observation of small diameter domes at the voltage pulse threshold suggests that these domes are intermediates in the formation of the pits that are observed at larger voltages in $H_2O(l)$ and at all voltages in humid air. This hypothesis was supported by the observation that in contact with $H_2O(l)$, domes could be

converted into 30-40 Å diameter pits by application of a sub-threshold, 0.2 V pulse. This indicates that the domes are metastable intermediates, and that they can be converted into pits with suitable physical or chemical stimuli. This also suggests that chemical reagents might be able to recognize these lithographically-produced metastable reactive sites and could yield specific reactions at predetermined positions on the HOPG surface.

Although the chemical structure of the domes has not been identified in this work, one possibility consistent with the available data is apparent from an energy minimized structure of a 15 carbon molecular analog of the graphite surface, in which one 6 carbon ring has been transformed from sp^2 (trigonal carbon) to sp^3 (tetrahedral carbon) hybridization (10). This calculation indicated that the sp^3 carbons puckered out of the graphite surface, producing a domed structure which had dimensions of 7 Å (dia.) and 0.45 Å (height). These dimensions are consistent with the observed dome size in Figure 1c. The rehybridization also produced a significant increase in the calculated bond angles for both these sp^3 carbons, and for the sp^2 carbons to which they are bonded. This strain energy also predicts that the domed features will exhibit enhanced reactivity relative to the pristine graphite surface, and such reactivity was observed experimentally in the ability to convert the domes to pits with a sub-threshold voltage pulse. While the exact mechanism responsible for the formation of the lithographic structures like that shown in Figure 1 can not be identified from the available data, an electrochemical mechanism seems unlikely in view of the observed polarity independence of the lithography process. Although the strain-induced structure represents one plausible candidate for a defect structure, Mizes and coworkers (11,12) and Soto (13) have predicted that a variety of defect types are capable of inducing an increase in the local density of states on graphite surfaces; thus alternative mechanisms can only be definitively ruled out when the chemical structures of the dome and pit features are available.

In conclusion, we have shown that STM-based lithography of HOPG in contact with $H_2O(l)$ is reproducible, leads to sub-nanometer diameter protrusions not observed previously in gaseous ambients, and leads to improved control over the pit diameter at larger voltage

pulses. Attempts to exploit these reactive features to achieve site-specific, nanometer-scale chemical derivatization of surfaces is under study at present.

Acknowledgements: We acknowledge the Caltech Consortium in Chemistry and Chemical Engineering; Foundind Members :E.I. du Pont de Nemours, Eastman Kodak, 3M, and Shell Development Co.and the Joint Services Electronics Program for support of this work, and Dr. A. Moore of Union Carbide for a generous donation of HOPG. J. Jahanmir at QuanScan Inc. is acknowledged for assistance with Z calibration of the piezo using interferometry. The authors also thank M. Dovek and M. Kirk of Stanford University for valuable conversations regarding experimental results in gaseous ambients. This is contribution #8201 from the Division of Chemistry and Chemical Engineering at Caltech.

References

a) Address correspondence to this author.

1. T.R. Albrecht, M.M. Dovek, M.D. Kirk, C.A. Lang, C.F. Quate, and D.P.E. Smith, Appl. Phys. Lett. **55**, 1727 (1989).

2. K. Terashima, M. Kondoh, and T. Yoshida, J. Vac. Sci. Technol. A **8**, 581 (1990).

3. J.P. Rabe, S. Buchholz and A.M. Ritcey, J. Vac. Sci Technol. A **8**, 679 (1990). H. Chang and A. J. Bard J. Am. Chem. Soc., **112**, 4598 (1990). W. Mizutani, J. Inukal, and M. Ono, Jap. J. Appl. Phys. **20**, L815 (1990).

4. Y.Z. Li, L. Vazques, R. Piner, R.P. Andres, and R. Reifenberg, Appl. Phys. Lett. **54**, 1424 (1989).

5. D.M. Eigler and E.K. Schweizer, Nature **344**, 524 (1990).

6. J.S. Foster, J.E. Foster, and P.D. Arnett, Nature **331**, 324 (1988).

7. M.M. Dovek, M.J. Heben, C.A. Lang, N.S. Lewis, and C.F. Quate Rev. Sci Instrum. **59**, 2333 (1988).

8. M.J.Heben, M.M. Dovek, N.S. Lewis, R.M. Penner, and C.F. Quate J. Microsc. **152**, 651 (1988).

9. Personal communications, Mike Kirk and Moris Dovek, June 1989.

10. Sp^3 carbons were positioned above the plane of the "graphite surface" prior to minimization to mimic the steric repulsion presented by an underlying graphite layer.

11. H.A. Mizes, S. Park, and W.A. Harrison, Phys. Rev. B **36**, 4491 (1987).

12. H.A. Mizes and W.A. Harrison, J. Vac. Sci, Technol. A **6**, 300 (1987).

13. M.R. Soto, Surf. Sci. **225**, 190 (1990).

Figure Captions

Figure 1 - STM images of pristine and lithographically modified HOPG in pure water. All images show derivative mode data obtained at a bias of -100 mV, a fast raster frequency (x direction) of 10 Hz, and a slow raster frequency (y direction) of 0.025 Hz.

a - HOPG surface in pure water prior to modification by lithography. Bright spots, corresponding to movement of the tip away from the surface, are graphite atoms separated by 2.46 Å.

b - Same region shown in Figure 1a following a reduction in sensitivity of the differential amplifier employed for derivative mode imaging.

c - Domed feature produced at HOPG in pure water using a -4.0 V x 20 μs bias pulse. Image window is 80 x 80 Å.

d - Cross sections of the domed feature shown in c.

e - Pit produced at HOPG in pure water using a -4.2 V x 20 μs bias pulse. Image window is 100 x 100 Å.

f - A cross section of the pit shown in e.

g - Large pit (dia. ≈ 80 Å) produced at HOPG in pure water using a -4.5 V x 20 μs pulse. Image window is 400 x 400 Å.

h - Cross sections of the large pit shown in g.

Figure 2 - Statistics for the feature diameter as a function of the bias pulse amplitude for lithography experiments at HOPG in water. Each data point represents 10 trials conducted with several polymer-coated tungsten tips over a seven day interval. Error bars are the calculated 1 σ confidence interval for these data.

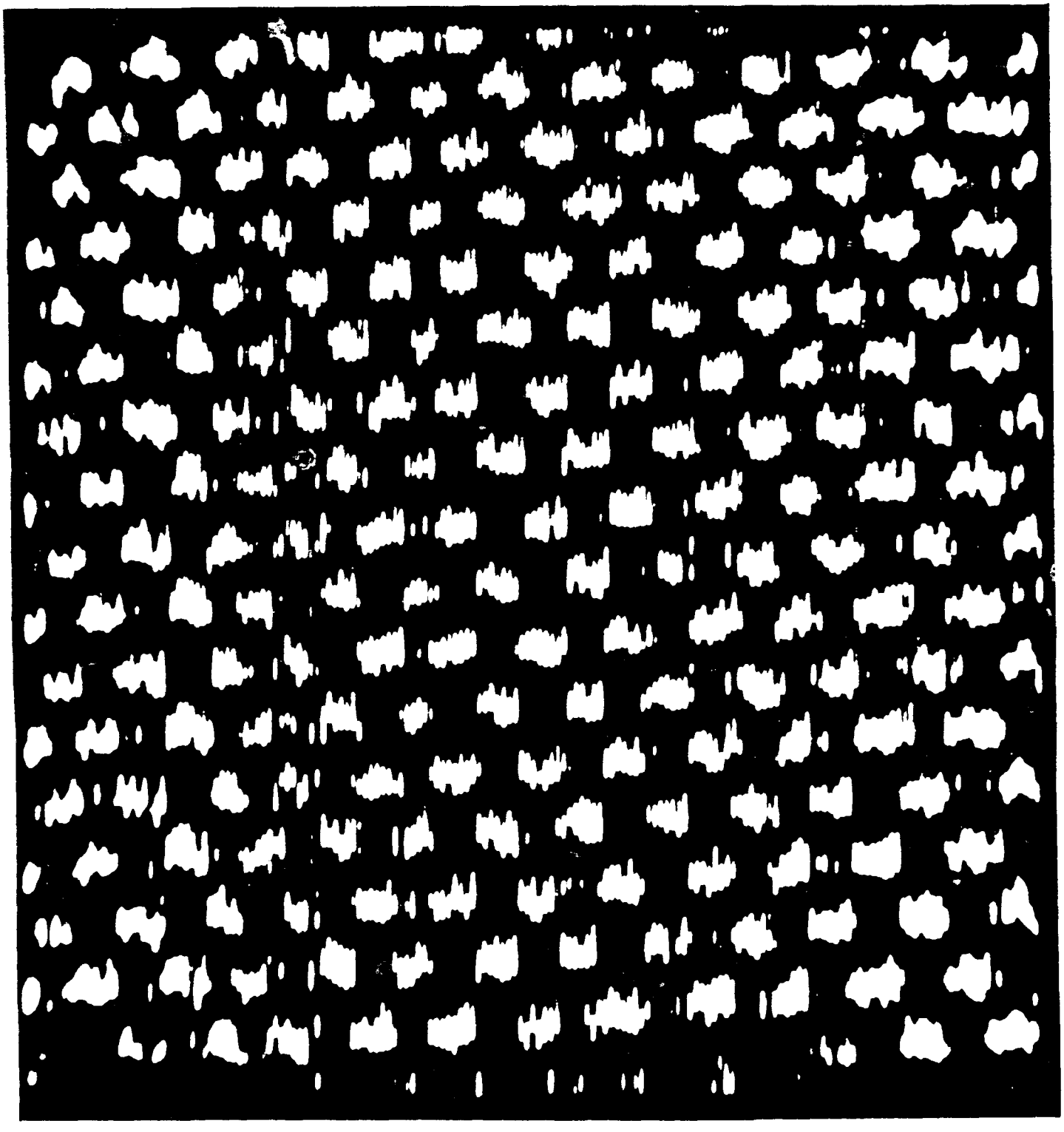

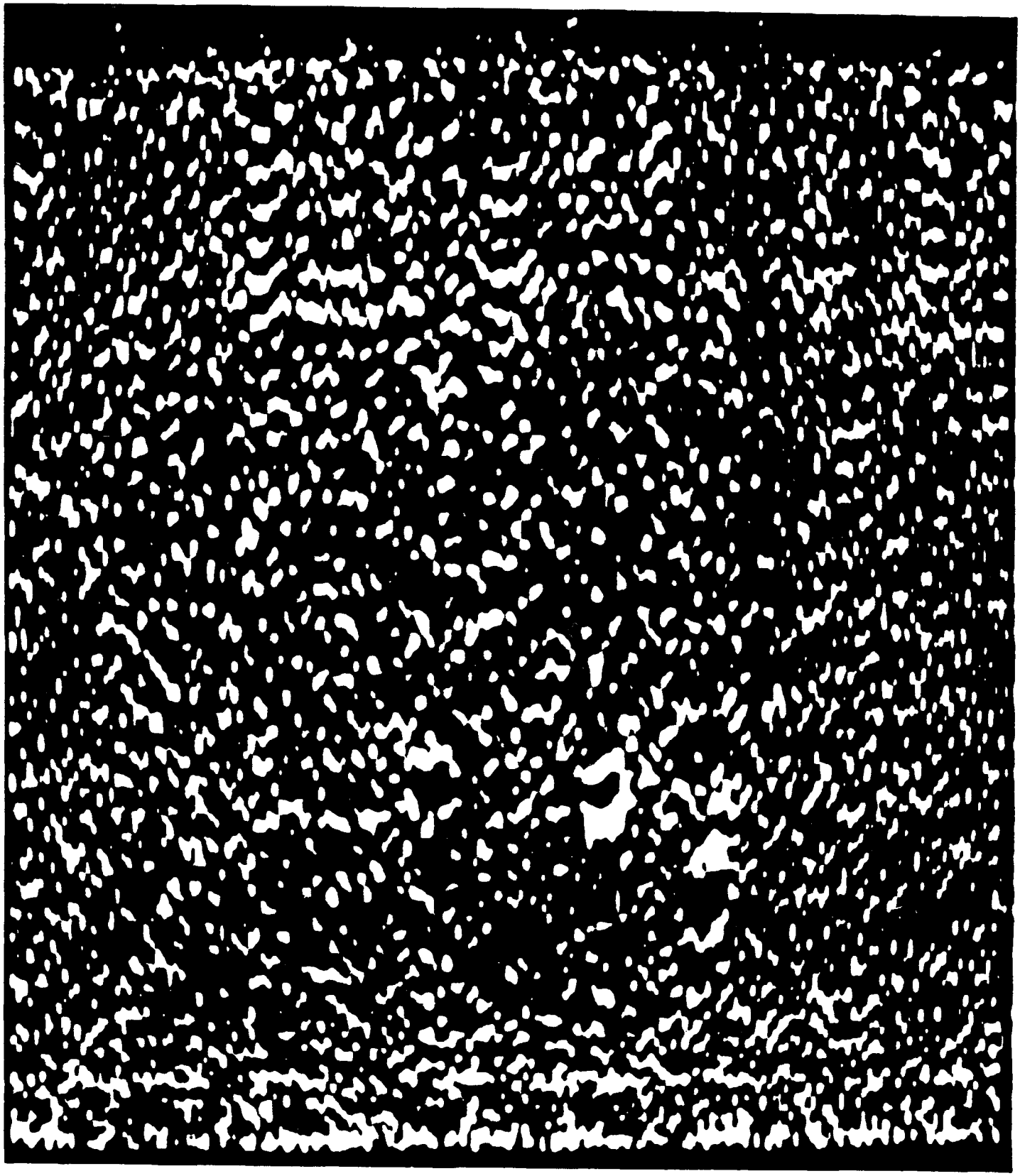

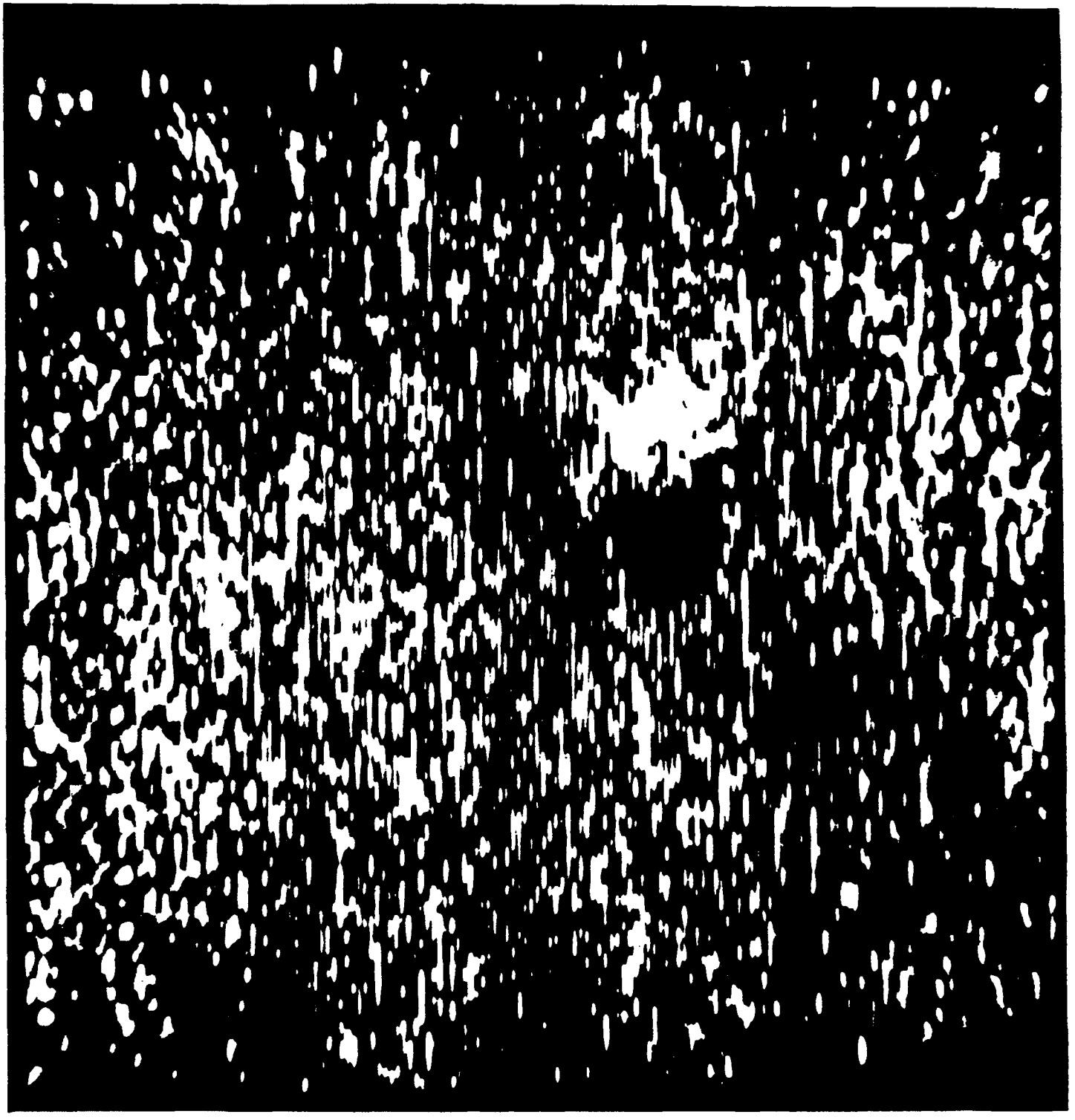

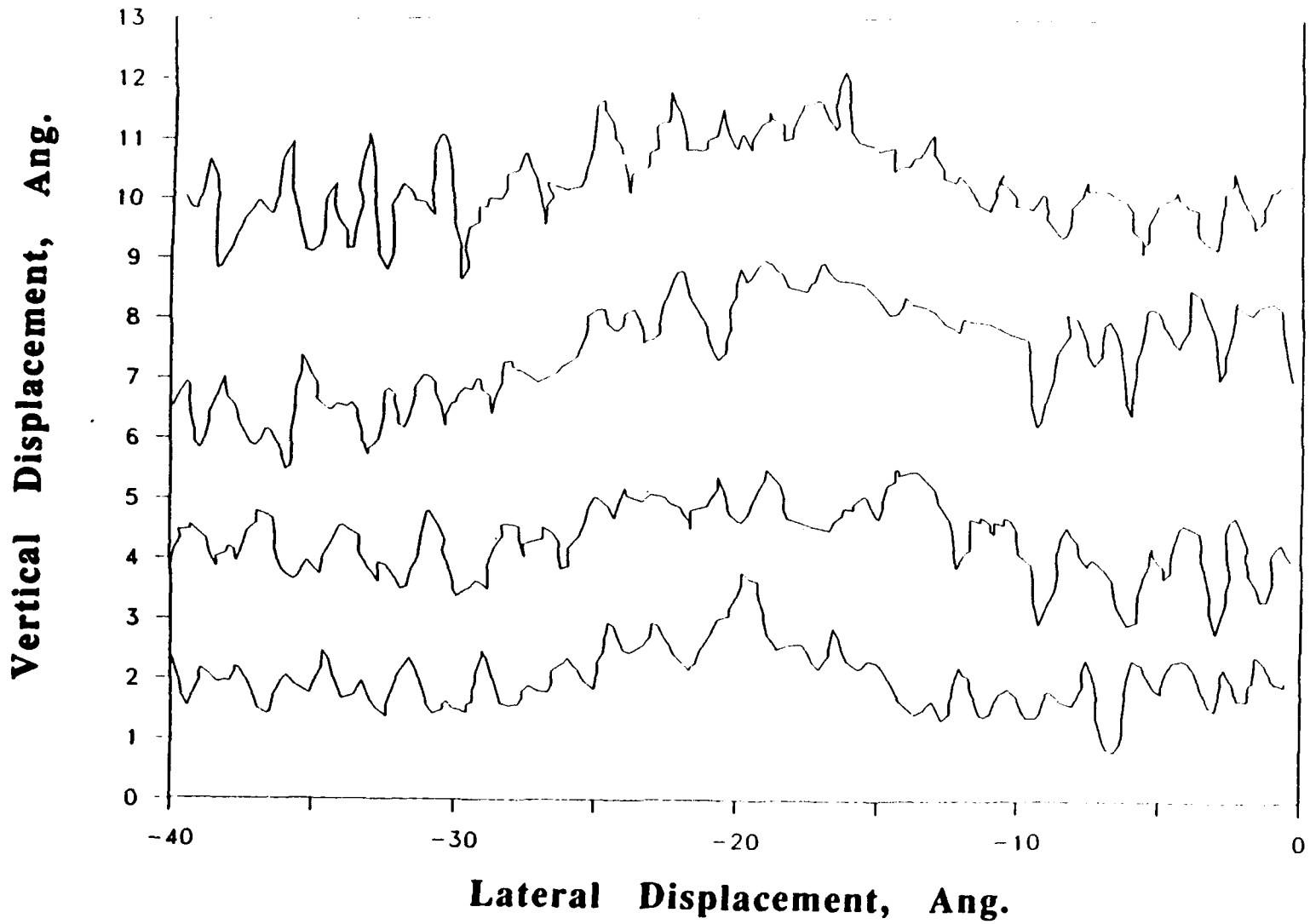
Vertical Displacement, Ang.
13
12
11
10
9
8
7
6
5
4
3
2
1
0
-40
-30
-20
-10
0
Lateral Displacement, Ang.

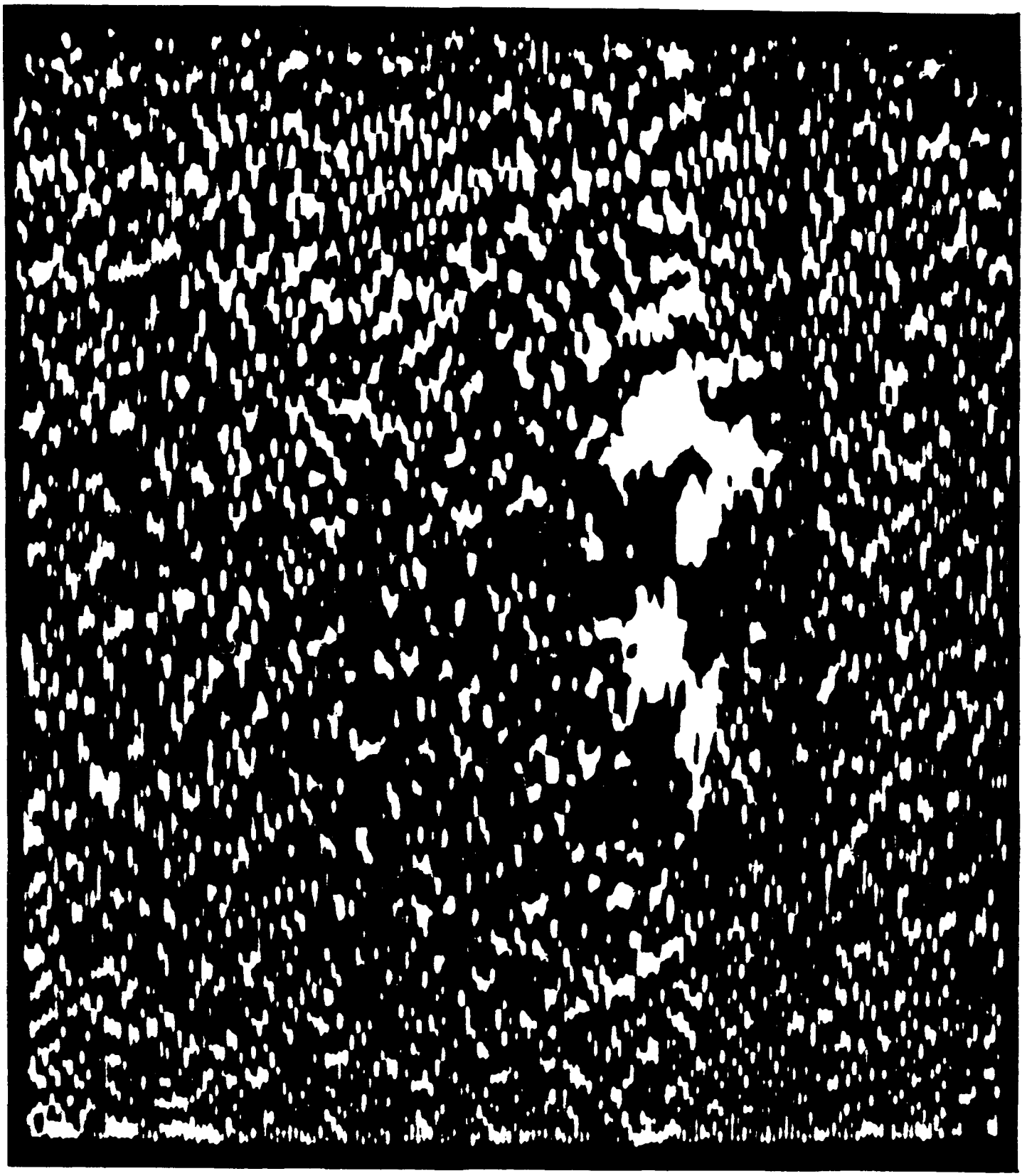

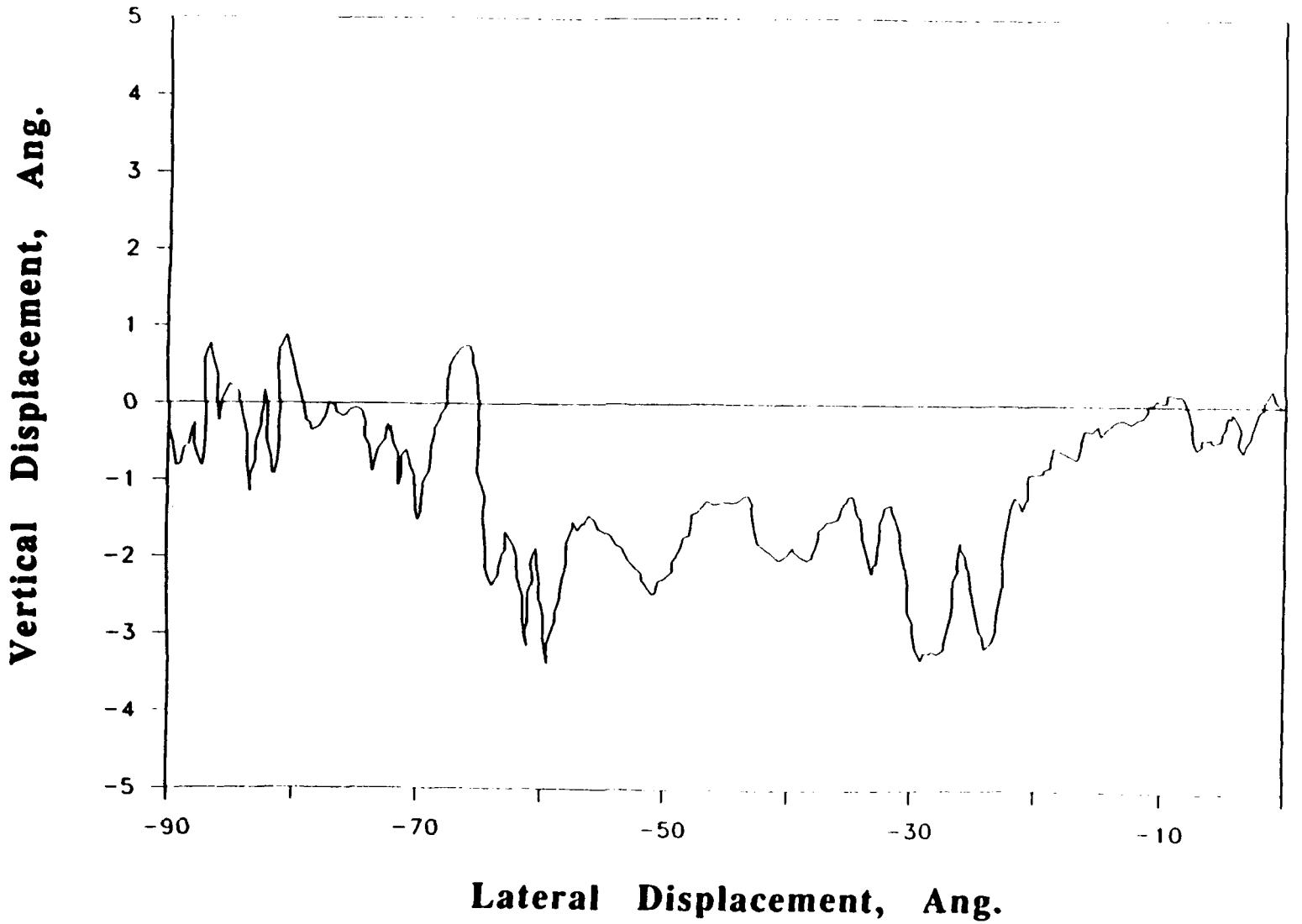
Vertical Displacement, Ang.
5
4
3
2
1
0
-1
-2
-3
-4
-5
-90
-70
-50
-30
-10
Lateral Displacement, Ang.

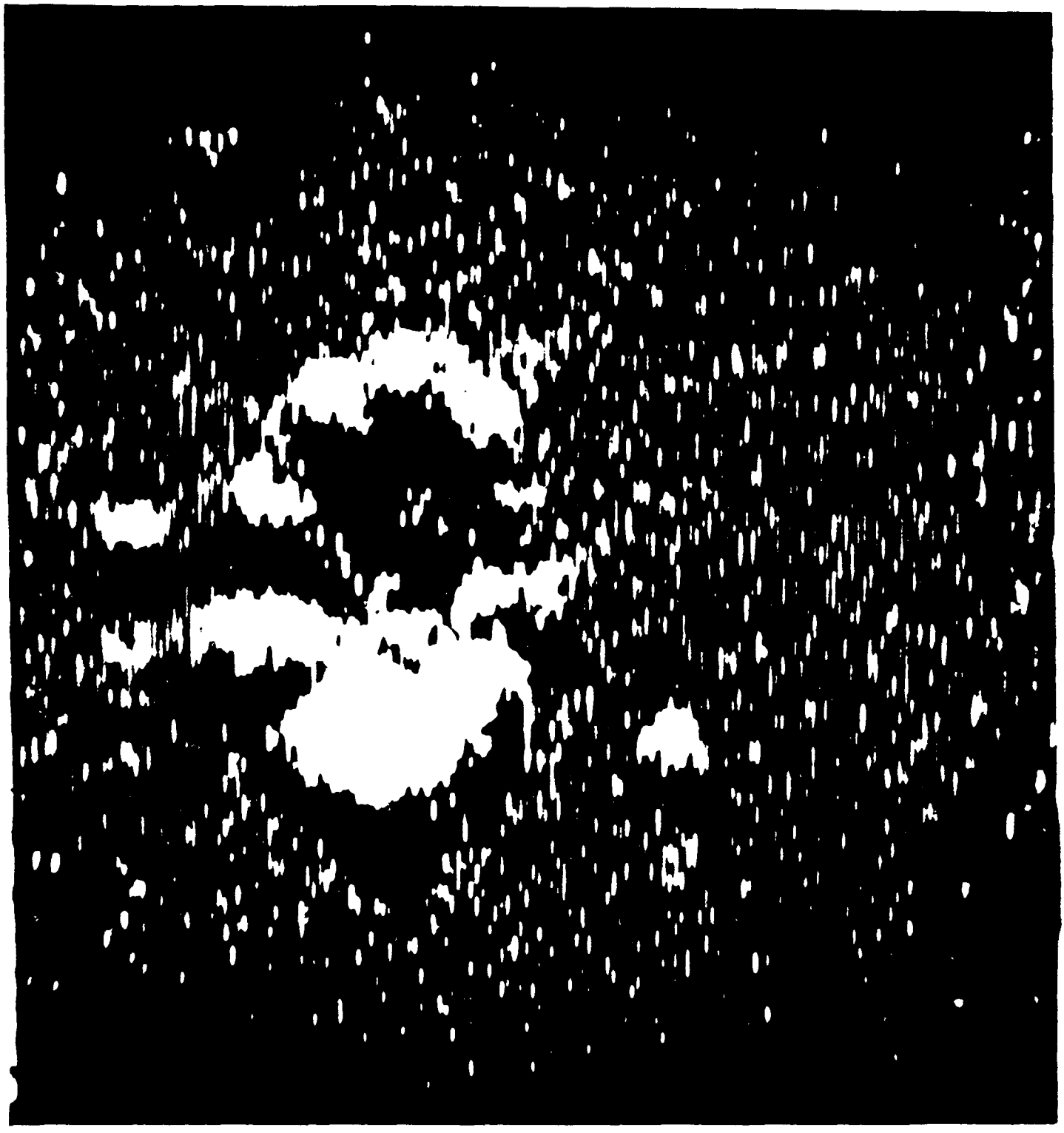

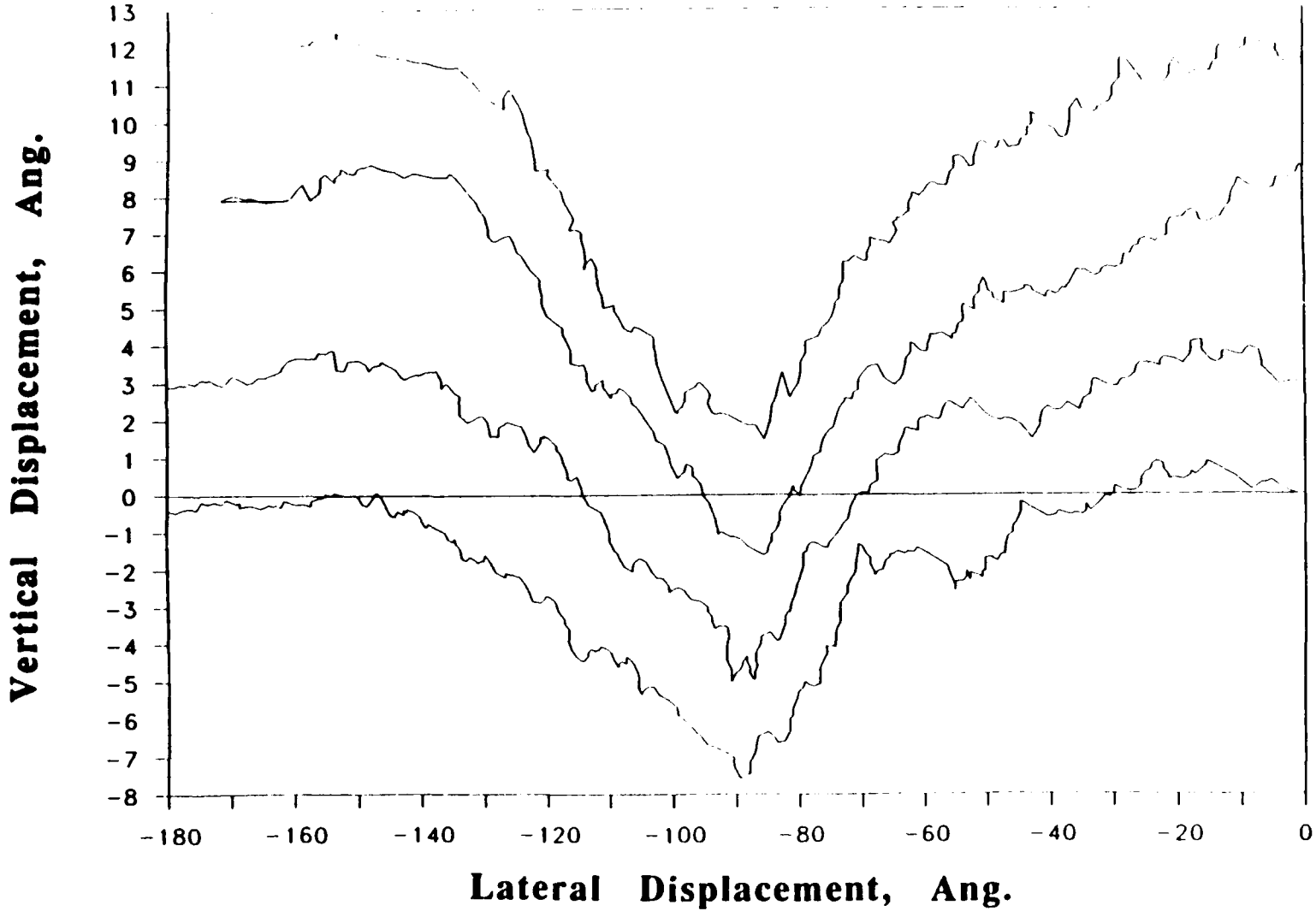
Vertical Displacement, Ang.
13
12
11
10
9
8
7
6
5
4
3
2
1
0
-1
-2
-3
-4
-5
-6
-7
-8
-180
-160
-140
-120
-100
-80
-60
-40
-20
0
Lateral Displacement, Ang.

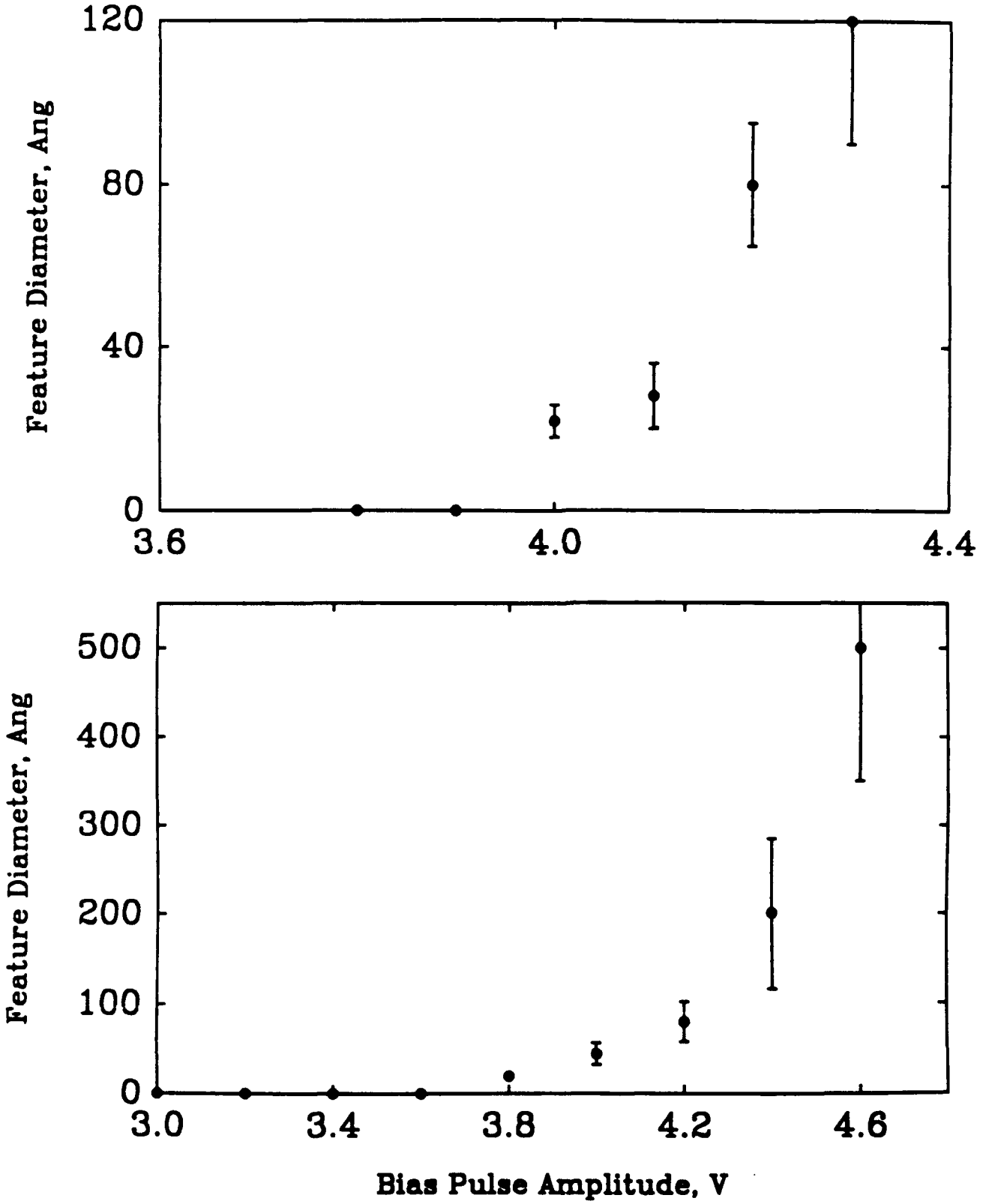
120
80
40
0
Feature Diameter, Ang
3.6
4.0
4.4
500
400
300
200
100
0
Feature Diameter, Ang
3.0
3.4
3.8
4.2
4.6
Bias Pulse Amplitude, V